# Supplementary Information for: *A shallow-water carbonate record of the Paleocene–Eocene Thermal Maximum from a Pacific Ocean guyot*

**Robinson, S.A.**

## 1. *Figure DR1. Present-day position of Limalok Guyot, ODP Site 871*

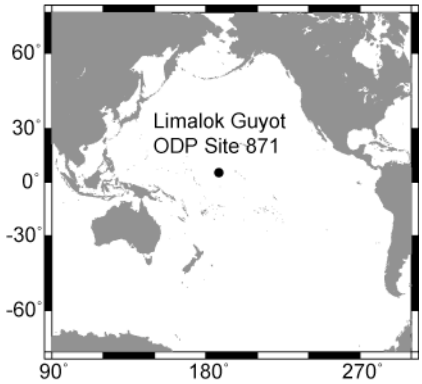


## 2. *Stable-isotope data*

### *2.1. Methods*

~1 $cm^3$ samples were taken every 5 cm where possible from Hole 871C (between ~420–130 mbsf) and bulk carbonate powder was extracted from these samples using a 0.5 mm drill bit, thereby homogenizing both matrix and cement (in a manner similar to the approach of Jenkyns and Wilson, 1999). Subsamples (~300–500 μg) of bulk powder were roasted at ~200 °C in a vacuum oven for 1 h and then analyzed for carbon and oxygen isotopes ($\delta^{13}C$, $\delta^{18}O$) using continuous flow isotope ratio mass spectrometry at the Bloomsbury Environmental Isotope Facility, University College London. All data are reported in the standard delta notation relative to VPDB. Reproducibility of an internal standard was ± 0.1‰ for both carbon and oxygen.

### *1.2. Results*

**Table DR1.** Carbon and oxygen isotope data from bulk carbonate.

| Sample (Core, section, interval) | Depth (mbsf) | $\delta^{13}C$ (‰, VPDB) | $\delta^{18}O$ (‰, VPDB) |
|---|---|---|---|
| ODP 144-871C- | | | |
| 2R-1, 5-6 | 133.75 | 1.2 | -1.3 |
| 2R-1, 15-16 | 133.85 | 1.5 | 0.0 |
| 2R-1, 20-21 | 133.90 | 1.2 | -2.0 |
| 2R-1, 25-26 | 133.95 | 1.4 | -1.5 |
| 2R-1, 30-31 | 134.00 | 0.9 | -4.6 |
| 2R-1, 35-36 | 134.05 | 1.4 | -1.0 |
| 2R-1, 40-41 | 134.10 | 1.3 | -1.4 |
| 2R-1, 45-46 | 134.15 | 1.1 | -1.4 |
| 2R-1, 55-56 | 134.25 | 0.7 | -3.2 |
| 2R-1, 60-61 | 134.30 | 1.1 | -2.8 |
| 2R-1, 65-66 | 134.35 | 1.1 | -3.7 |
| 4R-1, 5-6 | 152.95 | 1.5 | -2.1 |
| 4R-1, 10-11 | 153.00 | 1.7 | -1.6 |
| 4R-1, 20-21 | 153.10 | 2.2 | 0.6 |

| | | | |
|---|---|---|---|
| 4R-1, 25-26 | 153.15 | 1.6 | 0.5 |
| 4R-1, 30-31 | 153.20 | 1.4 | -3.5 |
| 4R-1, 35-36 | 153.25 | 0.6 | -3.1 |
| 4R-1, 40-41 | 153.30 | 0.8 | -2.2 |
| 4R-1, 45-46 | 153.35 | 1.0 | -2.0 |
| 4R-1, 50-51 | 153.40 | 1.3 | -1.3 |
| 5R-1, 0-1 | 162.60 | 1.5 | -0.9 |
| 6R-1, 0-1 | 172.30 | 1.5 | -0.6 |
| 6R-1, 5-6 | 172.35 | 1.5 | -1.4 |
| 6R-1, 15-16 | 172.45 | 1.4 | -2.2 |
| 6R-1, 20-21 | 172.50 | 0.9 | -2.5 |
| 6R-1, 30-31 | 172.60 | 0.8 | -2.1 |
| 6R-1, 35-36 | 172.65 | 1.0 | -1.6 |
| 6R-1, 40-41 | 172.70 | 1.0 | -1.4 |
| 6R-1, 45-46 | 172.75 | 1.0 | -1.6 |
| 6R-1, 50-51 | 172.80 | 1.0 | -1.9 |
| 6R-1, 55-56 | 172.85 | 1.1 | -1.8 |
| 8R-1, 0-1 | 191.50 | 1.4 | -3.3 |
| 8R-1, 5-6 | 191.55 | 0.7 | -2.2 |
| 8R-1, 10-11 | 191.60 | 1.4 | -0.4 |
| 8R-1, 15-16 | 191.65 | 1.5 | -3.3 |
| 9R-1, 0-1 | 201.20 | 1.7 | 0.1 |
| 9R-1, 5-6 | 201.25 | 0.7 | -3.7 |
| 9R-1, 15-16 | 201.35 | -0.8 | -3.8 |
| 9R-1, 20-21 | 201.40 | 0.6 | -5.3 |
| 9R-1, 25-26 | 201.45 | 0.5 | -4.8 |
| 9R-1, 30-31 | 201.50 | 2.0 | 0.2 |
| 9R-1, 35-36 | 201.55 | 0.8 | -1.7 |
| 9R-1, 40-41 | 201.60 | 1.0 | -1.5 |
| 10R-1, 0-1 | 210.90 | 1.6 | 0.0 |
| 10R-1, 5-6 | 210.95 | 1.8 | -0.4 |
| 10R-1, 10-11 | 211.00 | 0.6 | -4.2 |
| 10R-1, 15-16 | 211.05 | 1.9 | 0.5 |
| 11R-1, 0-1 | 220.50 | 1.3 | -0.6 |
| 12R-1, 0-1 | 230.10 | 1.5 | -1.5 |
| 12R-1, 5-6 | 230.15 | 0.9 | -2.1 |
| 13R-1, 0-1 | 239.80 | 1.2 | -1.2 |
| 13R-1, 5-6 | 239.85 | 0.9 | -1.1 |
| 14R-1, 0-1 | 249.50 | 1.3 | -1.5 |
| 14R-1, 5-6 | 249.55 | 1.0 | -1.3 |
| 14R-1, 20-21 | 249.70 | 1.0 | -1.6 |
| 15R-1, 0-1 | 259.20 | 1.2 | -3.0 |
| 15R-1, 5-6 | 259.25 | 0.8 | -3.2 |
| 15R-1, 10-11 | 259.30 | 1.1 | -3.2 |
| 15R-1, 15-16 | 259.35 | 0.7 | -3.3 |
| 15R-1, 20-21 | 259.40 | 1.0 | -2.9 |
| 16R-1, 1-2 | 268.81 | 0.6 | -2.9 |
| 16R-1, 5-6 | 268.85 | -0.2 | -3.8 |
| 16R-1, 11, 12 | 268.91 | 0.7 | -3.4 |
| 16R-1, 18-19 | 268.98 | 0.5 | -3.5 |
| 17R-1, 1-2 | 278.11 | -0.1 | -3.6 |
| 17R-1, 8-9 | 278.18 | 0.8 | -3.1 |
| 17R-1, 14-15 | 278.24 | 0.6 | -3.0 |
| 17R-1, 20-21 | 278.30 | 0.6 | -2.7 |
| 19R-1, 5-6 | 297.25 | -0.2 | -3.8 |
| 20R-1, 9-10 | 306.99 | 1.1 | -1.5 |
| 20R-1, 14-15 | 307.04 | 1.1 | -3.3 |
| 20R-1, 19-20 | 307.09 | 0.7 | -2.3 |

| | | | |
|---|---|---|---|
| 20R-1, 23-24 | 307.13 | 1.2 | -2.1 |
| 21R-1, 0-1 | 316.50 | 0.4 | -2.3 |
| 21R-1, 6-7 | 316.56 | 1.4 | -0.6 |
| 21R-1, 11-12 | 316.61 | 0.2 | -2.0 |
| 21R-1, 17-18 | 316.67 | 1.2 | -1.5 |
| 21R-1, 22-23 | 316.72 | 1.3 | -1.8 |
| 21R-1, 27-28 | 316.77 | 1.4 | -1.6 |
| 21R-1, 32-33 | 316.82 | 1.0 | -1.9 |
| 21R-1, 37-38 | 316.87 | 1.3 | -1.8 |
| 21R-1, 42-43 | 316.92 | 1.3 | -1.8 |
| 21R-1, 47-48 | 316.97 | 1.5 | -1.4 |
| 21R-1, 52-53 | 317.02 | 0.3 | -2.2 |
| 21R-1, 59-60 | 317.09 | 0.9 | -1.9 |
| 21R-1, 65-66 | 317.15 | 1.5 | -1.2 |
| 21R-1, 70-71 | 317.20 | 1.5 | -1.6 |
| 21R-1, 74.5-75.5 | 317.25 | 1.5 | -0.9 |
| 21R-1, 80-81 | 317.30 | 1.5 | -0.9 |
| 21R-1, 86.5-87.5 | 317.37 | 1.4 | -0.8 |
| 21R-1, 92-93 | 317.42 | 1.5 | -1.0 |
| 21R-1, 97-98 | 317.47 | 1.0 | -1.4 |
| 21R-1, 103-104 | 317.53 | 0.4 | -2.0 |
| 21R-1, 110.5-111.5 | 317.61 | 1.3 | -2.0 |
| 21R-1, 115-116 | 317.65 | 1.5 | -1.6 |
| 21R-1, 120-121 | 317.70 | 0.5 | -2.2 |
| 21R-1, 125-126 | 317.75 | 1.4 | -1.6 |
| 21R-1, 128-129 | 317.78 | 1.0 | -1.4 |
| 21R-1, 131.5-132.5 | 317.82 | 1.5 | -1.9 |
| 21R-1, 136.5-137.5 | 317.87 | 1.5 | -1.9 |
| 21R-1, 140-141 | 317.90 | 1.6 | -1.7 |
| 21R-2, 1-2 | 317.94 | 1.5 | -1.9 |
| 21R-2, 5-6 | 317.98 | 1.6 | -1.4 |
| 21R-2, 9-10 | 318.02 | 1.5 | -1.8 |
| 21R-2, 13-14 | 318.06 | 1.5 | -1.6 |
| 21R-2, 18-19 | 318.11 | 1.6 | -1.4 |
| 22R-1, 1-2 | 326.21 | 1.0 | -0.8 |
| 22R-1, 6-7 | 326.26 | 1.4 | 0.4 |
| 22R-1, 12-13 | 326.32 | 1.0 | -1.3 |
| 22R-1, 17-28 | 326.37 | 1.3 | -1.1 |
| 22R-1, 22-23 | 326.42 | 0.7 | -1.2 |
| 22R-1, 33-34 | 326.53 | 1.0 | -1.6 |
| 23R-1, 0-1 | 335.80 | 1.5 | -1.7 |
| 23R-1, 5-6 | 335.85 | -1.3 | -3.8 |
| 23R-1, 10-11 | 335.90 | -0.6 | -2.8 |
| 23R-1, 15-16 | 335.95 | -0.5 | -2.6 |
| 23R-1, 20-21 | 336.00 | 0.2 | -0.4 |
| 23R-1, 25-26 | 336.05 | -0.6 | -1.5 |
| 23R-1, 30-31 | 336.10 | 0.9 | 0.7 |
| 23R-1, 35-36 | 336.15 | 0.9 | 0.8 |
| 23R-1, 40-41 | 336.20 | 1.3 | -1.8 |
| 23R-1, 50-51 | 336.30 | 1.6 | -1.2 |
| 23R-1, 55-56 | 336.35 | 1.6 | -0.8 |
| 23R-1, 60-61 | 336.40 | 1.7 | -0.7 |
| 24R-1, 0-1 | 345.40 | 0.8 | -2.3 |
| 25R-1, 0-1 | 355.10 | 1.8 | -0.4 |
| 25R-1, 5-6 | 355.15 | 1.9 | -1.2 |
| 25R-1, 10-11 | 355.20 | 1.8 | -1.1 |
| 25R-1, 15-16 | 355.25 | 1.6 | -1.2 |
| 25R-1, 25-26 | 355.35 | 1.6 | -1.0 |

| | | | |
|---|---|---|---|
| 26R-1, 5-6 | 364.75 | 1.8 | -1.1 |
| 27R-1, 0-1 | 374.30 | 1.7 | -1.5 |
| 27R-1, 5-6 | 374.35 | 1.8 | -1.2 |
| 28R-1, 0-1 | 383.70 | 1.6 | -1.1 |
| 28R-1, 5-6 | 383.75 | 1.7 | -0.8 |
| 28R-1, 10-11 | 383.80 | 1.5 | -1.4 |
| 28R-1, 15-16 | 383.85 | 2.0 | -0.9 |
| 28R-1, 20-21 | 383.90 | 2.1 | -0.9 |
| 28R-1, 25-26 | 383.95 | 1.6 | -1.3 |
| 28R-1, 30-31 | 384.00 | 1.9 | -0.9 |
| 28R-1, 35-36 | 384.05 | 2.0 | -0.8 |
| 28R-1, 40-41 | 384.10 | 2.0 | -0.9 |
| 28R-1, 60-61 | 384.30 | 2.1 | -1.0 |
| 28R-1, 65-66 | 384.35 | 2.1 | -1.3 |
| 28R-1, 70-71 | 384.40 | 2.0 | -1.5 |
| 28R-1, 75-76 | 384.45 | 1.8 | -1.1 |
| 28R-1, 80-81 | 384.50 | 2.0 | -0.8 |
| 28R-1, 85-86 | 384.55 | 2.0 | -0.8 |
| 28R-1, 90-91 | 384.60 | 1.9 | -1.1 |
| 28R-1, 95-96 | 384.65 | 1.9 | -0.6 |
| 28R-1, 100-101 | 384.70 | 1.8 | -0.7 |
| 28R-1, 105-106 | 384.75 | 2.0 | -0.9 |
| 28R-1, 110-111 | 384.80 | 1.9 | -0.2 |
| 28R-1, 115-116 | 384.85 | 1.6 | -1.2 |
| 28R-1, 120-121 | 384.90 | 1.9 | -1.0 |
| 28R-1, 125-126 | 384.95 | 1.9 | -0.5 |
| 28R-1, 130-131 | 385.00 | 2.0 | -0.9 |
| 29R-1, 0-1 | 393.40 | 1.8 | -1.1 |
| 29R-1, 10-11 | 393.50 | 1.4 | -1.1 |
| 29R-1, 15-16 | 393.55 | 1.5 | -1.1 |
| 29R-1, 20-21 | 393.60 | 2.0 | -1.1 |
| 29R-1, 30-31 | 393.70 | 2.3 | -1.5 |
| 30R-1, 5-6 | 403.15 | 2.3 | -1.5 |
| 30R-1, 10-11 | 403.20 | 2.3 | -1.2 |
| 30R-1, 15-16 | 403.25 | 1.7 | -1.1 |
| 30R-1, 35-36 | 403.45 | 2.3 | -1.4 |
| 30R-1, 40-41 | 403.50 | 2.3 | -1.5 |
| 30R-1, 45-46 | 403.55 | 2.4 | -1.4 |
| 30R-1, 50-51 | 403.60 | 2.4 | -1.5 |
| 30R-1, 60-61 | 403.70 | 2.3 | -1.1 |
| 30R-1, 65-66 | 403.75 | 2.5 | -1.4 |
| 30R-1, 70-71 | 403.80 | 2.1 | -1.3 |
| 30R-1, 75-76 | 403.85 | 1.9 | -1.4 |
| 30R-1, 80-81 | 403.90 | 1.0 | -3.1 |
| 30R-1, 90-91 | 404.00 | 1.9 | -0.9 |
| 30R-1, 95-96 | 404.05 | 1.9 | -1.1 |
| 30R-1, 100-101 | 404.10 | 2.2 | -1.4 |
| 30R-1, 110-111 | 404.20 | 2.1 | -1.5 |
| 30R-1, 115-116 | 404.25 | 2.0 | -0.8 |
| 30R-1, 120-121 | 404.30 | 2.0 | -0.9 |
| 31R-1, 10-11 | 412.90 | 1.2 | -1.1 |
| 31R-1, 15-16 | 412.95 | 2.2 | -1.1 |
| 31R-1, 20-21 | 413.00 | 2.1 | -1.6 |

**Figure DR2.** Stratigraphy of ODP Hole 871C showing core recovery, lithological details, biostratigraphic summaries and carbon and oxygen isotope data. Lithological and biostratigraphic data from: 1: Premoli Silva et al., (1993); 2: Watkins et al., (1995); 3: Nicora et al., (1995).

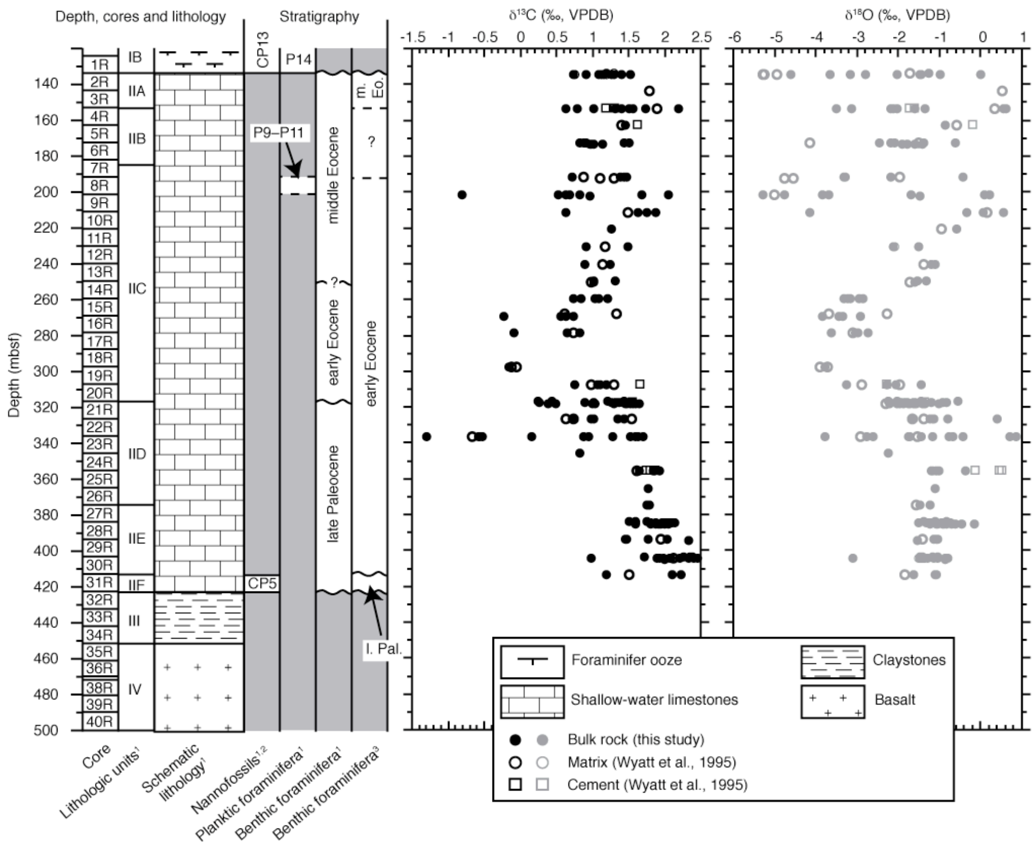

## *2. Age models*

The biostratigraphy and age models are based upon calcareous nannoplankton, planktonic foraminifera and larger benthic foraminifera (Premoli Silva et al. 1993; Nicora et al., 1995; Watkins et al., 1995). Previous assessments of the biostratigraphy of the platform have suggested that the carbonate platform is of Late Paleocene–Eocene. Nannofossils assigned to zone CP5 (late Paleocene) are present close to the base of the platform in Core 144-871C-31R-1 (Premoli Silva et al., 1995), while the oldest pelagic sediment above the platform is of middle Eocene age (nannofossil zone CP13 occurs in sample 144-871A-15H-CC, 10-13 cm); Watkins et al., 1995). The depth at which these samples occur has been assigned an age based on the midpoint of the age range implied by the zonal assignment (Table DR2). Ages are taken from Gradstein et al. (2004). By approximating the age of each sample, it is possible to construct a very simple age model based on linear interpolation between the two datums thereby providing a first approximation to the age-depth relationship (Figure DR2). Further age models can be constructed by assigning ages to samples with diagnostic specimens of larger benthic and planktonic foraminifera (from Nicora et al., 1995), based upon the mid-point of the zonal age range implied by those specimens (Table DR2 and Figure DR2). The three age models used are:

*Age model 1:* This age model simply assumes a linear accumulation rate between the two nannofossil datums at the top and bottom of the carbonate platform. Age = (Depth+749.16)/19.786, where Age is in Ma and Depth in meters below sea floor.

*Age model 2:* This age model is based on a linear regression through all of the biostratigraphic datums. Age = (Depth+770.51)/19.978, where Age is in Ma and Depth in meters below sea floor. This relationship has an $r^2$ value of 0.92302.

*Age model 3:* Given the Jurassic age of the underlying crust (Premoli Silva et al., 1993) thermal subsidence of the platform might have followed an exponential relationship, like ‘old’ ocean crust (Parsons and Sclater, 1977). Thus this age model is based on an exponential regression through all of the biostratigraphic datums. Age = ln(Depth/3.2551)/0.083584, where Age is in Ma and Depth in meters below sea floor. This relationship has an $r^2$ value of 0.90094.

To assign ages to the benthic foraminiferal data of Nicora et al., (1995) the shallow benthic zonation of Serra-Kiel et al., (1998) has been used in conjunction with the timescale of Gradstein et al., (2004). Recent results (Pujalte et al., 2009; Scheibner and Speijer, 2009) adjusting the relative timing of the SBZ zones and the Paleocene–Eocene boundary (as defined by the CIE) have also been incorporated.

All the age models predict that the Paleocene–Eocene boundary should be between ~340 to 355 mbsf, close to the negative carbon-isotope excursion observed in Core 23R at ~336 mbsf. This prediction is in contrast to a previous study that indicated an almost entirely Eocene age for the carbonate platform (Nicora et al., 1995). This age assignment was based upon the occurrance of *Alveolina* sp. and *Asterocyclina* sp. in, respectively, cores 144-871C-32R, -26R, -25R and core 144-871C-29R, although both these genera are present in the Late Paleocene (see BouDagher-Fadel, 2008). At this level of identification these samples could not be included in the age model. Furthermore, a late Paleocene age for the basal part of the carbonate platform is strongly suggested by the presence in Core 144-871C-21R (~317 mbsf), of a nummulitic benthic foraminifera thought to be very similar to *Nummulites deserti* (Nicora et al. 1995). *N. deserti* occurs in SBZ5 and SBZ6 (Serra-Kiel et al. 1998) constraining the age of Core 21R to the first ~800 kyrs of the Eocene. Given the likely subsidence rates of Limalok Guyot (between 20 and 30 m/Myr) this would strongly suggest that the basal 100 m of the platform must extend into the Late Paleocene, as suggested by the nannofossils.

**Table DR2.** Data used to construct the age models for Site 871. Biostratigraphic data from Premoli Silva et al., (1993), Nicora et al., (1995), and Watkins et al., (1995); zonal assignments for larger benthic foraminifera from Serra-Kiel et al. (1998); age assignments from Gradstein et al. (2004).

| Datum | Bottom sample (core, section, interval) | Top sample (core, section, interval) | Average Depth (mbsf) | Zone | Max. age (Ma) | Min. age (Ma) | Av. Age (Ma) |
|---|---|---|---|---|---|---|---|
| **Nannofossils** | | | | | | | |
| CP13 | 15H-CC, 10-13 | | 133.70 | CP13 | 46.57 | 42.66 | 44.62 |
| CP5 | 31R, 47-48 | | 413.28 | CP5 | 59.17 | 58.32 | 58.75 |
| **Larger benthic foraminifera** | | | | | | | |
| *Nummulites* sp. cf. *N. laevigatus* | 2-1, 51-54 | 2-1, 44-50 | 134.20 | SBZ13 | 48.60 | 45.44 | 47.02 |
| *Nummulites nitidus* group | 9-1-CC | | 201.20 | SBZ11 | 50.66 | 49.12 | 49.89 |
| *Alveolina pinguis* | 15-1, 15-20 | | 259.38 | mid SBZ11–SBZ12 | 49.89 | 48.60 | 49.25 |
| *Alveolina ilerdensis* & *A.* aff. *Ilerdensis* | 20-1, 13-18 | 19-1, 3-9 | 302.16 | late SBZ8–SBZ10 | 53.735 | 51.745 | 52.74 |
| *Alveolina* sp. *A. sakaryaensis* | 20-1, 13-17 | 19-1-4, 10 | 302.16 | SBZ7–SBZ8 | 55.09 | 53.09 | 54.09 |
| *Nummulites* sp. cf *N. deserti* | 21-1, 72-77 | 21-1, 17-20 | 316.97 | SBZ5–SBZ6 | 55.80 | 55.09 | 55.45 |

Note: all samples are from Hole 871C, with the exception of the nannofossils assigned to zone CP13, which are from Hole 871A, but is assigned the depth of the Mn crust in Hole 871C.

**Figure DR3.** Age models for the carbonate platform sediments of Site 871, see text for details. The thermal subsidence curve is shown to illustrate the idealised subsidence curve for Limalok Guyot, if it had followed the young crust subsidence curve of Parsons and Sclater (1977). This curve places a maximum on the possible rates of subsidence, which were clearly much slower (see Larson et al., 1995). Biostratigraphy from Gradstein et al. (2004) and modified around PETM using Pujalte et al. (2009) and Scheibner & Speijer (2009).

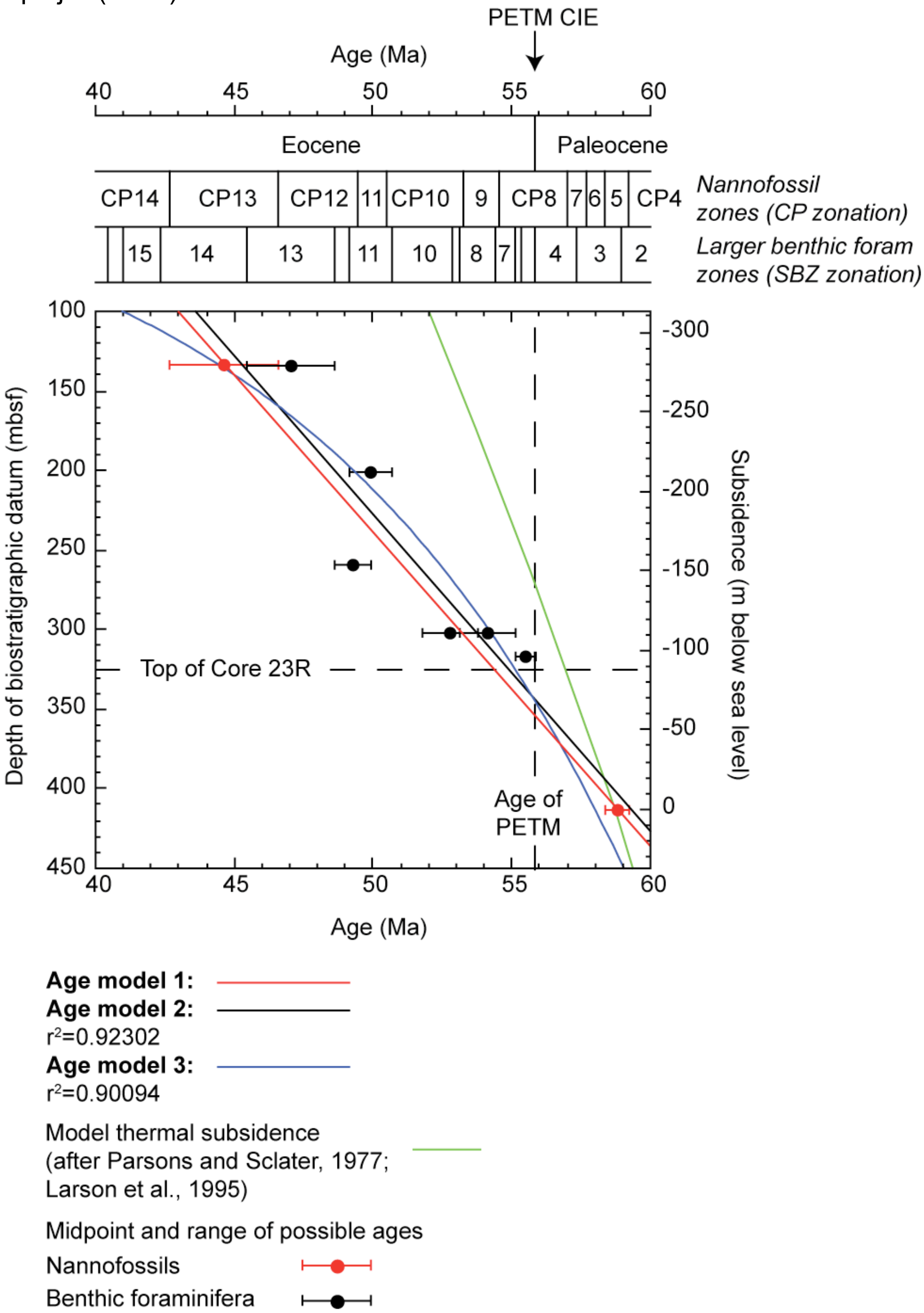

### *3. Carbon isotope data against age*

**Figure DR4.** Comparison between a deep-sea benthic foraminiferal $\delta^{13}C$ stacked curve (Zachos et al., 2008) and $\delta^{13}C$ data from Site 871, plotted using three different age models. It should be noted that the age of the PETM differs between the age models used for Site 871 (55.8 Ma) and the deep-sea compilation (~55 Ma), due to recent updates to the GTS (Gradstein et al., 2004), and new data on the relative timing of larger benthic foraminiferal zones and the carbon-isotope excursion (Pujalte et al., 2009; Scheibner & Speijer, 2009). In order to make the two age models broadly comparable for the purposes of this study the Zachos et al (2008) data have been plotted with an offset of 0.8 Myrs.

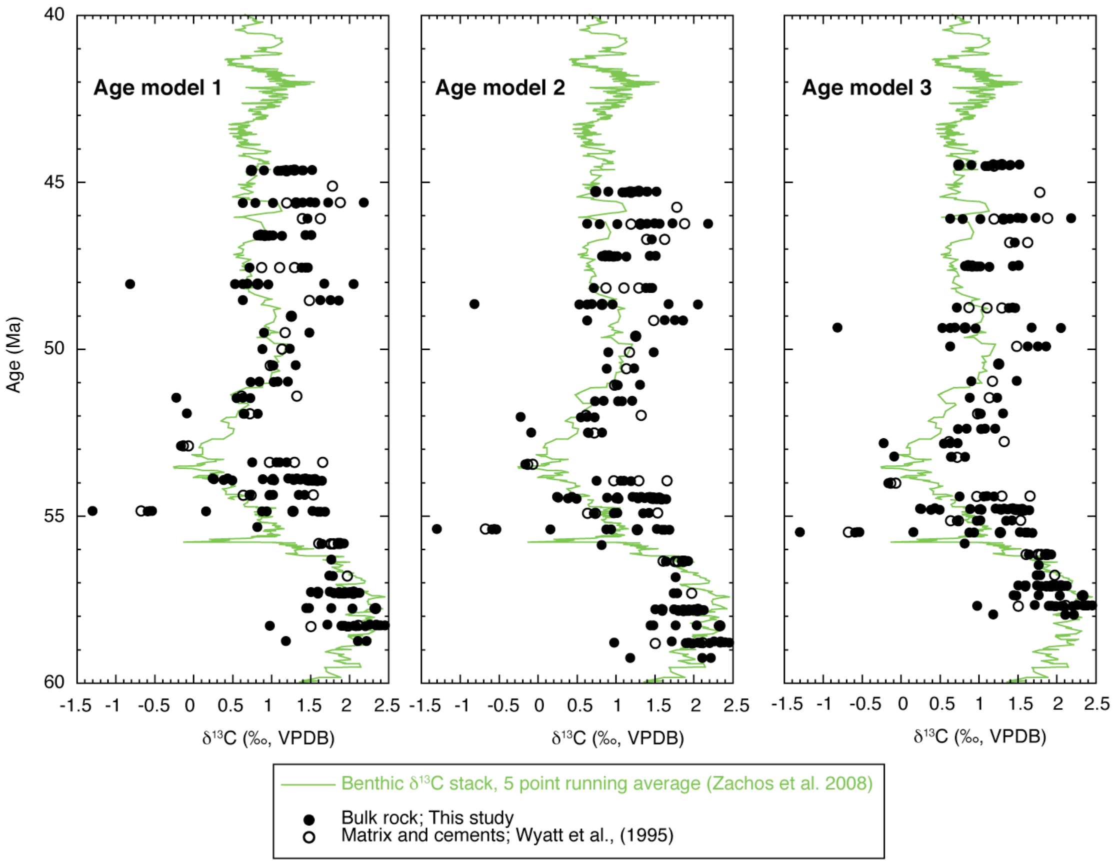

## 4. References

BouDagher-Fadel, M.K., 2008, Evolution and geological significance of larger benthic foraminifera, Developments in Palaeontology and Stratigraphy, v. 21, Elsevier, Amsterdam, The Netherlands.

Gradstein, F.M., Ogg, J.G., and Smith, A.G., 2004, *A Geologic Time Scale*, 2004. Cambridge University Press, Cambridge, UK.

Larson, R.L., Erba, E., Nakanishi, M., Bergersen, D., and Lincoln, J.M., 1995, Stratigraphic, vertical subsidence and paleolatitude histories of Leg 144 guyots, *in* Premoli-Silva, I., Haggerty, J., Rack, F., et al., Proceedings of the Ocean Drilling Program, Scientific Results, v. 144, College Station, TX (Ocean Drilling Program), p. 915-933.

Nicora, A., Premoli Silva, I., and Arnaud Vanneau, A., 1995, Paleogene larger foraminifer biostratigraphy from Limalok Guyot, Site 871, *in* Premoli-Silva, I., Haggerty, J., Rack, F., et al., Proceedings of the Ocean Drilling Program, Scientific Results, v. 144, College Station, TX (Ocean Drilling Program), p. 127-139.

Parsons, B., and Sclater, J.G., 1977, An analysis of the variation of ocean floor bathymetry and heat flow with age: Journal of Geophysical Research, v.82, p. 803-829.

Premoli-Silva, I., Haggerty, J., Rack, F., and the Shipboard Scientific Party, 1993, Proceedings of the Ocean Drilling Program, Initial Reports, v. 144, College Station, TX (Ocean Drilling Program).

Pujalte, V., Baceta, J.I., Schmitz, B., Orue-Etxebarria, X., Payros, A., Bernaola, G., Apellaniz, E., Caballero, F., Robador, A., Serra-Kiel, J., and Tosquella, J., 2009, Redefinition of the Ilerdian Stage (early Eocene): Geologica Acta, v. 7, p. 177-194.

Scheibner, C., and Speijer, R.P., 2009, Recalibration of the Tethyan shallow-benthic zonation across the Paleocene-Eocene boundary: the Egyptian record: Geologica Acta, v. 7, p. 195-214.

Serra-Kiel, J., Hottinger, L., Caus, E., Drobne, K., Ferrandez, C., Jauhri, A.K., Less, G., Pavlovec, R., Pignatti, J., Samso, J.M., Schaub, H., Sirel, E., Strougo, A., Tanbareau, Y., Tosquella, J., and Zakrevskaya, E., 1998, Larger foraminiferal biostratigraphy of the Tethyan Paleocene and Eocene: Bulletin de la Société Géologique de France, v. 169, p. 281-199.

Watkins, D.K., Premoli Silva, I., and Erba, E., 1995, Cretaceous and Paleogene manganese-encrusted hardgrounds from central Pacific guyots, *in* Premoli-Silva, I., Haggerty, J., Rack, F., et al., Proceedings of the Ocean Drilling Program, Scientific Results, v. 144, College Station, TX (Ocean Drilling Program), p. 97-126.

Wyatt, J.L., Quinn, T.M., and Davies, G.R., 1995, Preliminary investigation of the petrography and geochemistry of limestones at Limalok and Wodejebto Guyots (Sites 871 and 874), Republic of the Marshall Islands, *in* Premoli-Silva, I., Haggerty, J., Rack, F., et al., Proceedings of the Ocean Drilling Program, Scientific Results, v. 144, College Station, TX (Ocean Drilling Program), p. 429-437.

Zachos, J.C., Dickens, G.R., and Zeebe, R.E., 2008, An early Cenozoic perspective on greenhouse warming and carbon-cycle dynamics: Nature, v. 451, p. 279-283.